JACS
JOURNAL OF THE AMERICAN CHEMICAL SOCIETY

Communication

pubs.acs.org/JACS

# Patterned Silver Nanoparticles embedded in a Nanoporous Smectic Liquid Crystalline Polymer Network

Debarshi Dasgupta,[†,▽,#] Ivelina K. Shishmanova,[†,#] Amparo Ruiz-Carretero,[†] Kangbo Lu,[‡] Martinus Verhoeven,[§] Huub P. C. van Kuringen,[†] Giuseppe Portale,[∥] Philippe Leclère,[⊥] Cees W. M. Bastiaansen,[†] Dirk J. Broer,[†] and Albertus P. H. J. Schenning*[,†]

[†]Laboratory of Functional Organic Materials and Devices, [‡]Laboratory of Materials and Interface Chemistry, Cryo-TEM Unit, and [§]Laboratory of Inorganic Materials, Eindhoven University of Technology, P.O. Box 513, 5600 MB, Eindhoven, The Netherlands

[∥]Netherlands Organization for Scientific Research (NWO), European Synchrotron Radiation Facility (ESRF), DUBBLE-CRG, Grenoble, F-38043, France

[⊥]Laboratory for Chemistry of Novel Materials, Center for Innovation and Research in Materials and Polymers (CIRMAP), University of Mons (UMONS), Place du Parc 20, B 7000 Mons, Belgium

Supporting Information

**ABSTRACT:** A nanoporous smectic liquid crystalline polymer network has been exploited to fabricate photo patternable organic−inorganic hybrid materials, wherein, the nanoporous channels control the diameter and orientational order of the silver nanoparticles.

Nanoporous materials are of great current interest due to their application in areas, such as filtration, separation, and catalysis.[1] Due to the small pore size in these materials, discrimination between molecules and ions based on size and shape is possible, while the confined environment enhances chemical reactions and product selectivity. For the fabrication of such materials, the self-organization of liquid crystals (LCs) and their polymers is appealing since the pore size can be decreased to 1 nm and below.[1,2]

Nanoporous architectures, such as metal−organic frameworks, protein cages, and nanotubes, have recently also attracted considerable attention as host materials for inorganic nanoparticles to make shape-controlled structures.[3] For the fabrication of these hybrid materials, nanoporous liquid crystalline polymer networks present an attractive organic medium, having well-defined and uniform pores and long-range orientational order. Furthermore in such systems, the appealing properties of nanoparticles and nanoporous materials can be combined. Liquid crystalline polymers have been used to prepare hybrid materials,[4,5] however, the use of nanoporous liquid crystalline materials has not been explored yet.

Recently we have reported on nanoporous hydrogel films based on smectic LCs consisting of hydrogen-bonded benzoic acid moieties and a cross-linker (**1**, **2**, Figure 1).[6] Swelling of these films at high pH is highly anisotropic and expansion mainly takes place in the plane of the smectic layers.[7] We now show that these anisotropic hydrogels can be used as nanoporous materials to make silver nanoparticles hybrid structures. Silver nanoparticles were chosen since they can be made (photo)chemically and have interesting catalytic, surface enhanced Raman scattering and antimicrobial and antiviral properties.[8] The anisotropic nanoporous gel is fabricated first and subsequently filled with silver ions. After chemical reduction of the silver ions, a lamellar polymer hybrid film is obtained that contains silver nanoparticles in which the particle diameter is controlled by the length of the cross-linker (**2** vs **3**, stretched molecular length is roughly 4 and 5.5 nm, respectively, Figure 1). By using a photomask, the silver ions can also be photochemically converted to silver nanoparticles yielding patterned polymer films where the unexposed pores are still accessible.

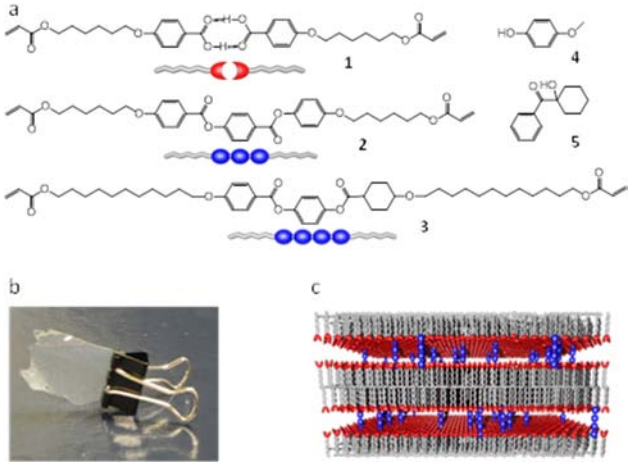


**Figure 1.** (a) Chemical structures of the hydrogen-bonded LC dimer **1**, the two cross-linkers **2**, **3**, inhibitor **4**, and photoinitiator **5**. (b) Freestanding planar aligned smectic LC film based on **1** and **2**. (c) Schematic representation of the smectic nanoporous polymer film. It should be noted that in reality the orientation of benzoic acid units in the nanoporous film is random. In a planar alignment the plane of the smectic layers is parallel to the thickness of the film.

The anisotropic polymer hydrogel was fabricated by photopolymerizing the reactive hydrogen-bonded LC dimer **1** containing a small amount of mesogenic cross-linker **2** (Figure 1) in the smectic A phase as previously reported.[6,7] An 18 $\mu$m

**Received:** May 21, 2013
**Published:** July 8, 2013

   dx.doi.org/10.1021/ja404825y | J. Am. Chem. Soc. 2013, 135, 10922−10925

thick monodomain free-standing polymer planar aligned smectic film (Figure 1, Figure S1) was fabricated using a cell having polyimide alignment layers. Subsequently, the film was placed for 24 h in an alkaline $Na_2B_4O_7$/NaOH buffer at pH = 10 to break up the hydrogen bonds and open the pores (Figure 2). The resulting polymer sodium salt formation was confirmed by Fourier transform infrared spectroscopy (FT-IR) (Figure S2).[7,9]

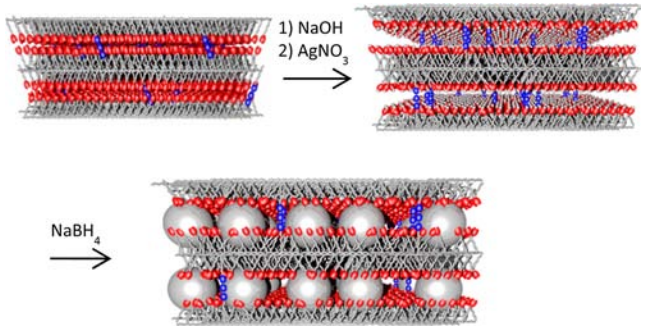


**Figure 2.** Schematic representation of the fabrication method of the silver nanoparticles containing nanoporous smectic liquid crystalline polymer network. In step one the LC film is treated with base to open the pores. Subsequently, the pores are filled with silver ions that, upon reduction with sodium borohydride, form silver nanoparticles. It is proposed that the cross-linker determines the size of the pores and therefore the size of the silver nanoparticles.

The nanoporous polymer sodium salt hydrogel was immersed overnight in a 0.1 M $AgNO_3$ solution to replace the $Na^+$ ions by $Ag^+$ ions (Figure 2). Excess of surface adsorbed $Ag^+$ ions was subsequently removed by an additional rinsing step. The FT-IR spectra (Figure S2) of the dried film before and after $Ag^+$-treatment look similar, exhibiting the characteristic features of carboxylate anions. X-ray photoelectron spectroscopy (XPS) measurements revealed (Figure S3, S4) a Ag-3d doublet appearing at 368.08 eV ($3d_{5/2}$) and 374.05 eV ($3d_{3/2}$), showing that the polymer film contains $Ag^+$ ions.[10] Apart from the top layer, the binding energies remain unchanged through the depth XPS scans revealing the presence of silver ions in the entire film. Thermogravimetric analysis shows that the content of inorganic fraction is 28 wt %, which is close to the theoretically calculated fraction (32%) assuming complexation of two $Ag^+$ ions per hydrogen-bonded mesogenic dimer **1** revealing that each carboxylate contains one silver ion (Figure S5). The silver salt polymer film exhibited a birefringence (Figure S6) similar to the polymer sodium salt film.

The smectic polymer silver salt film serves as the precursor for the size-controlled synthesis of silver ($Ag^0$) nanoparticles by treating the film with an aqueous sodium borohydride ($NaBH_4$) solution (Figure 2).[11] XPS measurements showed a change of the binding energy spectrum indicating the reduction of $Ag^+$ to $Ag^0$ (Figures 3 and S7). The binding energies measured in $Ag^+$-salt film give slightly higher values as compared to those measured for the corresponding $Ag^0$ film (e.g., $3d_{5/2}$ = 367.88 eV and $3d_{3/2}$ = 373.85 eV). The decrease in Ag-3d binding energy is consistent with reduction of $Ag^+$ to $Ag^0$. In addition, the XPS depth profile (Figures S7, S8) shows that the Ag-3d binding energy remains constant all-throughout from surface to near bulk, revealing the reduction of $Ag^+$ through the entire polymer film.

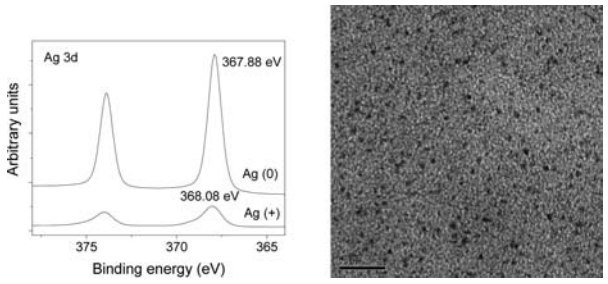


**Figure 3.** Left-hand side, XPS Ag-3d region scans showing the difference in binding energy between the $Ag^0$ and $Ag^+$ **1**, **2** hybrid films. Right-hand side, TEM image of an ultramicrotomed cross-section of a planar aligned $Ag^0$ smectic **1**, **2** hybrid film (scale bar 20 nm).

Transmission electron microscopic (TEM) study of a cryo-ultramicrotomed cross-section of the planar aligned $Ag^0$ polymer LC film discloses (Figure 3) the formation of uniformly distributed silver nanoparticles having diameters 1.3 ± 0.2 nm. Moreover, the size distribution indicates nearly monodisperse nanoparticle formation (Figure S9). Previous studies have shown that upon uptake of ions, the cross-linker is uniaxially oriented perpendicular to the smectic layer and keeps the layers together in the polymer film.[6] The benzoic acid groups become randomly oriented after breaking of the hydrogen bonds, and it was estimated that in case of cross-linker **2**, the periodicity is roughly 3 nm, and pore size is close to 1 nm.[6] The growth of the nanoparticles is most likely arrested by the confined space of the nanopores as well as the carboxylate groups which act as capping agents.[12] The fact that the diameter of the particles is somewhat larger than the pore size is probably due to the flexibility of the benzoylate units. Presumably, spherical nanoparticles are formed instead of anisotropic sheets due to the relatively low concentration of silver ions as a result of the stoichiometric complexation of $Ag^+$ with the gallery carboxylates in the pores (Figure 2).[13] It should be noted that the TEM image of the cross-sectional microtomed slice of the planar aligned polymer films alone does not show an orientational order of the silver nanoparticles (*vide infra*).

The effect of confined nanocrystallization has been further investigated in a similar smectic network having the longer cross-linker **3** instead of **2** (Figure 1). The binary mixture of **1** and **3** also exhibits a smectic mesophase (Figure S10). TEM analysis of cross-sectional cryo-microtomed planar **1**, **3** film treated with barium ions revealed layered morphology with a periodicity of ∼4.5 nm (Figure S11, S12), which is longer than found earlier in the LC films containing cross-linker **2**. The film is also less ordered than found earlier, indicating a more flexible polymer film.

After using the same fabrication method as used for the **1**, **2** polymer films (Figure 2), the silver nanoparticles containing polymer films with longer cross-linker **3** were analyzed by TEM. The cross-sectional TEM images of the planar aligned LC show the presence of silver nanoparticles having now a larger average diameter of 5.4 nm (Figure 4). The particle size distribution (5.4 ± 0.8) nm is narrow, emphasizing the templating effect imparted by the nanogalleries. The particle diameter is larger than the length of cross-linker **3** which indicate that the polymer matrix is flexible.[14]

Further investigation of an ultra cryo-microtomed section of the silver nanoparticle LC **1**, **3** polymer film was performed by


dx.doi.org/10.1021/ja404825y | J. Am. Chem. Soc. 2013, 135, 10922−10925

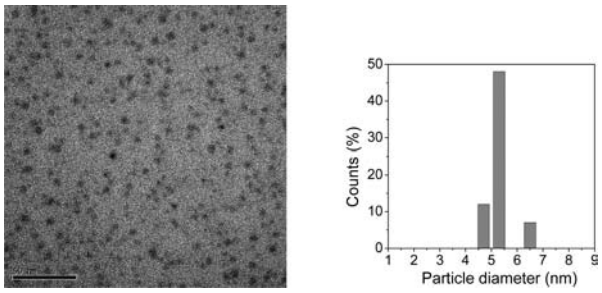


**Figure 4.** TEM image along with the particle size distribution of an ultramicrotomed section of a planar $Ag^0$-smectic **1**, **3** hybrid film (scale bar 50 nm).

peak force tapping atomic force microscopy (PFT AFM, Figures S14, S15).[15] Remarkably, the deformation mapping (Figures 5a,b, S16) exhibits a layered morphology over a large

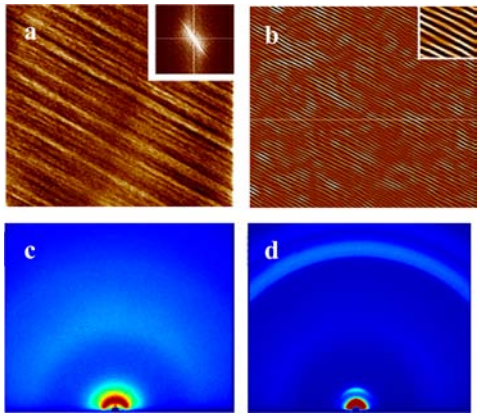


**Figure 5.** (a) PFT AFM deformation image (500 × 500 nm) of a cryo-microtomed section of a planar silver nanoparticle LC **1**, **3** polymer film, inset shows the FFT profile. (b) FFT refined image of deformation mapping showing the alternation of dark (less deformable) and bright (more deformable) layers of 7.5 nm. (c) GIXD 2D images of the **1**, **3** polymer $Ag^+$ salt film and (d) silver nanoparticle LC **1**, **3** polymer film.

cross sectional surface. The alternative dark layers residing in between bright layers correspond to less deformable (high modulus) material, pointing to the nanopores containing silver nanoparticles. The direction of the layers is perpendicular to the orientation of the molecular director (Figure 2).[16] To extract the quantitative information about layer spacing, a FFT-transformed micrograph (Figure 5a,b) is used giving more precise values of smectic layer thicknesses. The cumulative length measured of an inorganic−organic layer is 7.5 nm, which is much longer than periodicity found for the same polymers treated with barium ions (Figure S12). It could be that the cross-section cutting of the planar aligned was done under a larger angle which will result in longer distances (Figure S15). 2D gracing incidence X-ray diffraction (GIXD) measurements[17] on a homeotropic silver nanoparticle **1**, **3** polymer films confirmed the ordered layered structure with a typical spacing of 4.3 nm. In this sample, the polymer layers and nanopores are aligned parallel to the glass substrate as confirmed by the two arched sharp smectic reflections (Figures 5c,d, S17). The presence of $Ag^0$ nanoparticles in the LC films is confirmed by the (111) and (200) reflections visible above 20 $nm^{-1}$ (Figures 5d, S15). Moreover, the increased diffracted intensity at low $q$ values is due to the embedded nanoparticle scattering. The fact that TEM image of the silver nanoparticles polymer films does not exhibit such layered structure is most likely due to the poor in depth resolution in which the silver particles dominate the contrast.

We have also explored the fabrication of patterned hybrid polymer films. For this purpose a homeotropically oriented LC **1**, **2** polymer silver salt film was used as photoresponsive ink. This precursor film was exposed to UV irradiation through a chromium micropatterned mask.[18] In the irradiated parts, the bound $Ag^+$ ions were reduced to $Ag^0$ nanostructures. Optical microscopy shows micropatterned photographs taken in transmission mode that correspond to the mask pattern used (Figure 6a, c). A scanning electron microscopy image of the dot

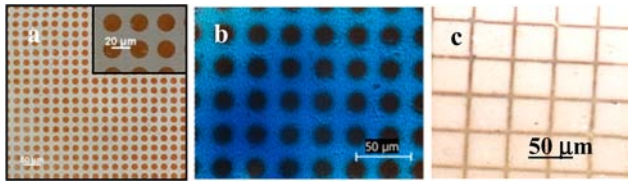


**Figure 6.** (a,c) Optical micrographic images of a photopatterned LC **1**, **2** polymer silver salt films. (b) Photopatterned LC **1**, **2** polymer silver salt film treated with Nile blue.

patterned hybrid film (Figure S18) shows the electron-rich bright dots of same dimensions as seen by optical microscopy corresponding to the $Ag^0$ areas. Interestingly, when the photopatterned films were treated with a Nile blue dye solution, the film becomes colored.[6] The optical micrograph (Figure 6b) clearly exhibits the incorporation of the blue dye distributed homogeneously within the polymer film, suggesting that the cationic dyes replace the cations in the film. This result shows that silver nanoparticles in the porous network structures are still accessible through the nanopores.

This work shows a novel approach toward a new class of organic−inorganic nanoporous materials involving the controlled synthesis of silver nanoparticles within a nanoporous smectic liquid crystalline polymer network. Our results show the profound effect of the covalent cross-linker on controlling the diameter of the silver nanoparticles. This strategy can in principle be extended to fabricate micropatternable anisotropic plasmonic or semiconducting hybrid structures. Preliminary experiments showed that the pores could also be filled with other metal ions (Figure S19). The nanoporosity of the hybrid polymer films makes them interesting for a wide variety of applications, ranging from nanoreactors to antimicrobial patches.

## ■ ASSOCIATED CONTENT

### Ⓢ Supporting Information

Experimental details and supporting data. This material is available free of charge via the Internet at http://pubs.acs.org.

## ■ AUTHOR INFORMATION

### Corresponding Author

a.p.h.j.schenning@tue.nl

### Present Address

[▽]Momentive Performance Materials, Survey No-9; Electronic City, Bangalore-560100, India.

### Author Contributions

[#]These authors contributed equally to this work.

### Notes

The authors declare no competing financial interests.

## ■ ACKNOWLEDGMENTS

We like to thank Bram Breugel for investigating the anisotropic swelling of the polymer films. This work was supported by the Eindhoven University of Technology and The Netherlands Organization for Chemical Research with financial aid from The Netherlands Organization for Scientific Research and the European Community within the Marie Curie program of Framework 7 (Hierarchy Project).

## ■ REFERENCES

(1) (a) Gin, D. L.; Lu, X.; Nemade, P. R.; Pecinovsky, C. S.; Xu, Y.; Zhou, M. *Adv. Funct. Mater.* **2006**, *16*, 865. (b) Kato, T. *Angew. Chem., Int. Ed.* **2010**, *49*, 7847. (c) Schenning, A. P. H. J.; Gonzalez-Lemus, Y. C.; Shishmanova, I. K.; Broer, D. J. *Liq. Cryst.* **2011**, *38*, 1627. (d) Broer, D. J.; Bastiaansen, C. M. W.; Debije, M. G.; Schenning, A. P. H. J. *Angew. Chem., Int. Ed.* **2012**, *51*, 7102.

(2) *Cross-linked Liquid Crystalline Systems*; Broer, D. J., Crawford, G. P., Zumer, S., Eds.; CRC Press, Taylor and Francis Group: Boca Raton, 2011.

(3) Examples: (a) Wie, Y.; Han, S.; Walker, D. A.; Fuller, P. E.; Grzybowski, B. A. *Angew. Chem., Int. Ed.* **2012**, *51*, 7435. (b) Eisele, D. M.; von Berlepsch, H.; Böttcher, C.; Stevension, K. J.; Vanden Bout, D. A.; Kristein, S.; Rabe, J. P. *J. Am. Chem. Soc.* **2010**, *132*, 2104. (c) Kasyutich, O.; Ilari, A.; Fiorillo, A.; Tatchev, D.; Hoell, A.; Ceci, P. *J. Am. Chem. Soc.* **2010**, *132*, 3621. (d) Reches, M.; Gazit, E. *Science* **2003**, *300*, 625.

(4) Use of liquid crystalline polymers containing inorganic nanoparticles: (a) Zadoina, L.; Soulantica, K.; Ferrere, S.; Lonetti, B.; Respaud, M.; Minogtaud, A.-F.; Falqui, A.; Genovese, A.; Chaudret, B.; Mauzac, M. *J. Mater. Chem.* **2011**, *21*, 6988. (b) Barmatov, E. B.; Pebalk, D. A.; Barmatova, M. V. *Langmuir* **2004**, *20*, 10868. (c) Barmatov, E. B.; Pebalk, D. A.; Barmatova, M. V. *Liq. Cryst.* **2006**, *33*, 1059. (d) Shandryuk, G. A.; Matukhina, E. V.; Vasilev, R. B.; Rebrov, A.; Bondarenko, G. N.; Merekalov, A. S.; Gaskov, A. M.; Talroze, R. V. *Macromolecules* **2008**, *41*, 2178. (e) Ezhov, A.; Shandryuk, G. A.; Bondarenko, G. N.; Merekalov, A. S.; Abramchuk, S. S.; Shatalova, A. M.; Manna, P.; Zubarev, E. R.; Talroze, R. V. *Langmuir* **2011**, *27*, 13353. (f) Gascon, I.; Marty, J.-D.; Gharsa, T.; Mingotaud, C. *Chem. Mater.* **2005**, *17*, 5228. (g) Liu, J.-H.; Yang, P.-C.; Chiu, Y.-H. *J. Polym. Sci., Part A: Polym. Chem.* **2006**, *44*, 5933. (h) Saliba, S.; Coppel, Y.; Achard, M.-F.; Mingotaud, C.; Marty, J.-D.; Kahn, M. L. *Angew. Chem., Int. Ed.* **2011**, *50*, 12032. (i) Zhao, D.; Zhou, W.; Cui, X.; Tian, Y.; Guo, L.; Yang. *Adv. Mater.* **2011**, *23*, 5779.

(5) Nonporous liquid crystalline systems containing noble metal nanoparticles: (a) Liu, Q.; Senyuk, B.; Tang, J.; Lee, T.; Qian, J.; He, S.; Smalyukh, I. I. *Phys. Rev. Lett.* **2012**, *109*, 088301. (b) Liu, Q.; Cui, y.; Gardner, D.; Li, X.; He, S.; Smalyukh, I. I. *Nano Lett.* **2010**, *10*, 1347. (c) Wojcik, M. M.; Gora, M.; Mieczkowski, J.; Romiszewski, J.; Goreckaa, E.; Pociecha, D. *Soft Matter* **2011**, *7*, 10561.

(6) Gonzalez, C. L.; Bastiaansen, C. W. M.; Lub, J.; Loos, J.; Lu, K.; Wondergem, H. J.; Broer, D. J. *Adv. Mater.* **2008**, *20*, 1.

(7) Shishmanova, I. K.; Bastiaansen, C. M. W.; Schenning, A. P. H. J.; Broer, D. J. *Chem. Commun.* **2012**, *48*, 4555.

(8) *Silver Nanoparticles: Properties, Characterization and Applications*; Welles, A. E., Ed.; Nova Science Pub Inc.: New York, 2010.

(9) Herzer, N.; Guneysu, H.; Davies, D. J. D.; Yildirim, D.; Vaccaro, A. R.; Broer, D. J.; Bastiaansen, C. W. M.; Schenning, A. P. H. J. *J. Am. Chem. Soc.* **2012**, *134*, 7608.

(10) Wagner, C. D., Riggs, W. M., Davis, C. E., Moulder, J. F., *Handbook of X-Ray Photoelectron Spectroscopy*; Muilenberg, G. E., Ed.; Perkin-Elmer: Eden Praire, MN, 1979.

(11) Wang, W.; Efrima, Regev, O. *Langmuir* **1998**, *14*, 602.

(12) Yook, J. Y.; Choi, G.-H.; Suh, D. H. *Chem. Comm* **2012**, *48*, 5001.

(13) We expect that during the chemical reduction reaction the amount of silver atoms in the films remains the same. The number of silver atoms in a particle of 1.3 nm is around 67 and for 5 nm 3830 (see SI). So the ratio of Ag particle/COOH groups is 1/67 and 1/3830 for polymers containing cross-linker **2** and **3**, respectively.

(14) It should be noted that during the preparation of the silver nanoparticles, anisotropic swelling of the polymer films takes place. For the polymer **1**, **2** and **1**, **3** films the swelling along the director is roughly 5% upon placing in a pH 10 buffer, while the expansion perpendicular to the director is 45−50% and 55−60%, respectively (see ref 7 and Figure S13). This difference will also affect the size of the particles.

(15) (a) Pittinger, B. *Quantitative Mechanical Property Mapping at the Nanoscale with PeakForce QNM*, Bruker Application Note AN 128; Bruker Nano Surfaces Divison: Santa Barbara, CA, 2010. (b) Tielemans, M.; Roose, P.; Ngo, C.; Lazzaroni, R.; Leclère, Ph. *Prog. Org. Coat.* **2012**, *75*, 560.

(16) Scanning direction of AFM tip is in the same direction as the molecular director in the liquid crystalline material (Figure S15).

(17) GIXD of the initial **1**, **3** polymer film revealed a smectic-C type structure with lattice spacing of 3.7 nm and tilt angle of 38° (Figure S17) in which the mesogens are oriented homeotropically as evidenced by the orientation of the signal at $q_y$ 15 $nm^{-1}$. Furthermore the diffractograms revealed that the average layer spacing in the polymer silver salt film is 3.5 nm, and only orientation of planes parallel to the substrate is present. No higher order peaks were visible, suggesting that the opening of the pores and the ion inclusion induces structural disorder. The mesogens are randomly oriented as no significant anisotropic signal in the wide angle region is observed (Figure S17).

(18) Sensitized photoreduction of silver ions: Satoa, T.; Onakaa, H.; Yonezawab, Y. *J. Photochem. Photobiol., A* **1999**, *127*, 83.